CARBON 87 (2015) 78–86

Available at www.sciencedirect.com

ScienceDirect

journal homepage: www.elsevier.com/locate/carbon

Engineering the metal–organic interface by transferring a high-quality single layer graphene on top of organic materials

Xuefei Feng [a,b,2], *Liang Zhang* [a,1,2], *Yifan Ye* [a], *Yong Han* [a], *Qian Xu* [a], *Ki-Jeong Kim* [c], *Kyuwook Ihm* [c], *Bongsoo Kim* [c], *Hans Bechtel* [d], *Michael Martin* [d], *Jinghua Guo* [d], *Junfa Zhu* [a,*]

[a] *National Synchrotron Radiation Laboratory and Collaborative Innovation Center of Suzhou Nano Science and Technology, University of Science and Technology of China, Hefei 230029, PR China*

[b] *State Key Laboratory of Functional Materials for Informatics, Shanghai Institute of Microsystem and Information Technology, Chinese Academy of Sciences, Shanghai 200050, PR China*

[c] *Beamline Research Division, Pohang Accelerator Laboratory, Pohang, Kyungbuk 790-784, South Korea*

[d] *Advanced Light Source, Lawrence Berkeley National Laboratory, Berkeley, CA 94720, USA*

ARTICLE INFO

Article history:
Received 10 November 2014
Accepted 29 January 2015
Available online 4 February 2015

ABSTRACT

We present a new method for transferring chemical vapor deposition (CVD)-grown graphene onto the surfaces of organic materials directly. Raman and near edge X-ray absorption fine structure measurements prove that high-quality and single layer graphene/organic thin films can be obtained with minimized impurity introduction. In-situ synchrotron radiation photoemission spectroscopy combined with ultraviolet photoelectron spectroscopy experiments demonstrate that the inserted graphene can not only act as a buffer layer to reduce the interfacial chemical reactions between the deposited Al and organic materials, but also tune the metal/organic interface electronic structure significantly. This new graphene transfer technique may have a great potential in the application of engineering the metal–organic interface properties, which is one of the key technologies for the optimal design and fabrication of organic electronic and optoelectronic devices.

1. Introduction

Single layer or multi-layer graphene is a promising material in the application of many organic-based devices, such as organic light-emitting diodes (OLEDs) [1–3], organic solar cells (OSCs) [4–8], and organic field-effect transistors (OFETs) [9–16], due to its high optical transparency, large electrical/thermal conductivity and chemical stability. Despite its prodigious potential, fabricating high-performance and low-cost graphene-involved devices still remains a great challenge.

* *Corresponding author.*
E-mail address: jfzhu@ustc.edu.cn (J. Zhu).

[1] Present address: Lehrstuhl für Physikalische Chemie II, Friedrich-Alexander-Universität Erlangen-Nürnberg, D-91058 Erlangen, Germany.

[2] These two authors contributed equally to this paper, and should share first authorship.

http://dx.doi.org/10.1016/j.carbon.2015.01.059
0008-6223/

One major impediment is how to transfer the as-grown high-quality graphene onto desired substrates with high fidelity. Although millimeter-size single-crystalline graphene can be produced using modified chemical vapor deposition (CVD) method on metal substrates [17–21], it is difficult to transfer it onto different target materials for device fabrication with minimum change of the morphology and electronic property of graphene [22–24].

One commonly used method for transferring graphene onto desired substrates is using poly(methyl methacrylate) (PMMA) or thermal release tape as the supporting transfer materials [25–27]. However, previous studies have shown that the organic residues remained on graphene surface and some additional defects were created due to tearing and ripping of graphene sheets during transfer process [28,29]. These problems can be partially solved through post transfer treatments, e.g., annealing to high temperature (400 °C) or rinsing in mixed organic solvents [30,31]. However, the above treatments are only applicable for graphene transferred onto inorganic substrates. For organic device fabrication where graphene needs to be transferred onto organic substrates, these methods are obviously not compatible because the organic materials may be damaged during heating to high temperature or dissolved in organic solvents. In addition, the fact that defects can be created after multi-step transfer process in this method is also a big issue that should be addressed [32,33].

In order to overcome the issues of graphene quality degradation during the transfer process using foreign supporting materials, many efforts have been attempted to obtain a high-quality graphene film on the substrates of interests. For example, recently Tamaoki et al. reported a simple method of transfer-free fabrication of a graphene field-effect transistor (GFET) array by using solid-phase patterned growth of graphene on a SiO_2/Si substrate [34]. While Meng et al. developed a novel top-emission OLED with copper/graphene composite anode without graphene transfer process [3]. However, despite these developments, the transfer-free methods have limited applications and are not suitable for fabricating devices that requires the graphene to be on top of organic materials.

Here, we report a simple and novel method for transferring graphene onto organic materials directly. With this method, no additional material is introduced during the transfer process. Raman mapping and near-edge X-ray absorption fine structure (NEXAFS) measurements confirm that highly ordered single layer graphene on top of organic materials (i.e., poly(3-hexylthiophene) (P3HT) and PMMA in this study) can be obtained with reduced defects and minimized contaminants. We then in-situ deposit a thin Al electrode material on the as-prepared graphene/P3HT film and investigate the interface structure of Al/graphene/P3HT using synchrotron radiation photoemission spectroscopy (SRPES) and ultraviolet photoelectron spectroscopy (UPS). The results clearly demonstrate that with the insertion of graphene layer, the unwanted chemical reactions between Al and P3HT are substantially suppressed during the interface formation. Besides, the Al/P3HT interface electronic structure was also tuned by inserting the single layer graphene buffer layer.

2. Experimental

2.1. Single layer graphene growth

Single layer graphene samples (1 in. × 2 in.) were synthesized on 25 μm thick Cu foils (99.98% purity, Sigma–Aldrich) via a conventional CVD method, following the procedure reported previously [8]. Briefly, after cleaning the Cu foils with acetone and isopropyl alcohol (IPA) to remove surface contaminants, the single-layered graphene was grown on top of the copper foils with a mixture of methane and hydrogen at a temperature of 1050 °C and a pressure of 4.4×10^{-1} Torr in a tube furnace. The size of graphene can be increased for fabricating large-size devices.

2.2. Graphene transfer onto organic films

The transfer procedure of graphene onto organic thin films is presented in Fig. 1. First, polymer/chloroform solution (20 mg/ml) was spin-coated on the graphene/Cu surface at 2000 rpm for 1 min in a nitrogen glove box. These polymer/graphene/Cu samples were annealed at 120 °C for 15 min to remove any possible solvent residues. Thereafter, the underlying Cu foil was etched away using etchant so-called copper etch CE-100 (Transene, LOT No. 101204) for 6 h. Then, the graphene/polymer films were rinsed in ultrapure water for three times (30 min for each) to remove the remaining etchants. Next, clean silicon (Si) wafers were put on top of the films and then were flipped over in the water slowly and carefully. After the graphene/polymer/Si samples were taken out of water, they were put in nitrogen atmosphere and dried overnight. Here, PMMA and P3HT were chosen as the organic materials and the graphene/PMMA/Si and graphene/P3HT/Si samples were characterized by Raman mapping and NEXAFS experiments, respectively. Note that the yield of the transfer process is related with the thickness of the polymer films. In this study, the thickness of polymer films is made to be no less than 100 nm to avoid possible break or wrinkling of graphene.

For comparison, we also prepared pure P3HT/Si and PMMA/Si samples by spin-coating the polymer/chloroform solutions onto Si wafers directly. These samples were treated in the same conditions as those samples with graphene. All samples were stored in an ultra-high vacuum chamber before measurements.

It should be mentioned that for device fabrication, the electrical contact properties and mechanical adhesion strengths between graphene/organic film and rigid substrates may be less than ideal after graphene transfer. Thus, pressing and annealing at mild temperature after this process may be needed for real device fabrication.

2.3. Characterization

Raman spectroscopy and Raman mapping experiments were performed using a LabRAM ARAMIS system from HORIBA Inc. A 50-timesobjective lens was used and the laser spot size was *ca.* 0.5 μm for the 532 nm excitation. The laser power at samples was set to be 0.1 mW to avoid laser-induced heating [35]. For Raman mapping, the sample was placed on a piezo

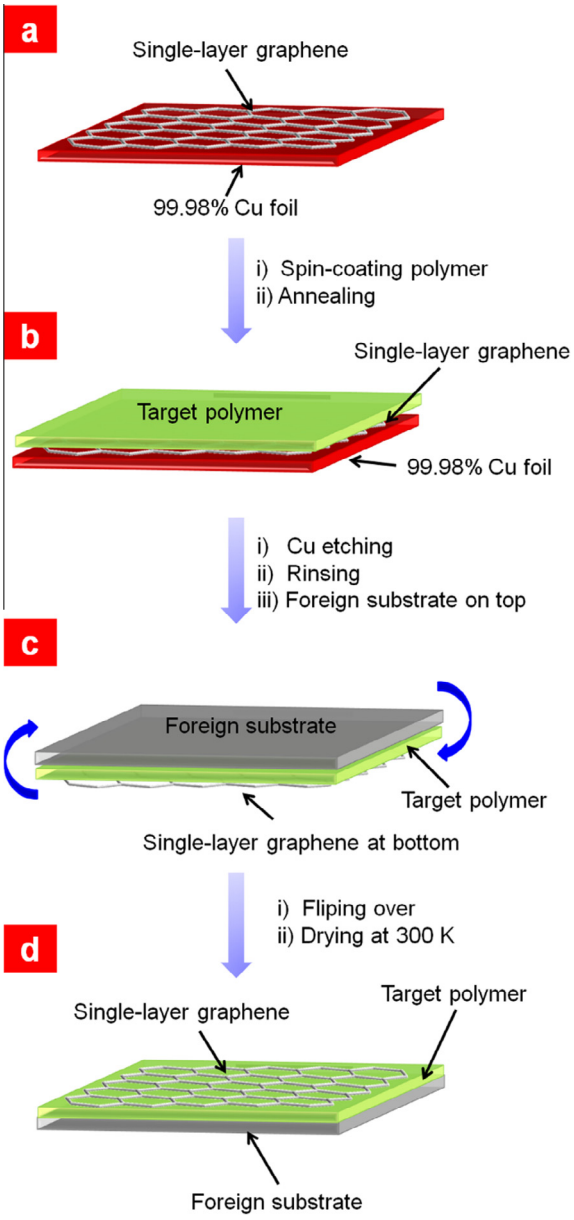

Fig. 1 – Schematic of transfer process of the single layer graphene onto target polymer organic materials. (a) Single layer graphene on Cu foil obtained by CVD growth, (b) spin-coating target polymer on single layer graphene, (c) after Cu etching, a foreign substrate (i.e., Si wafer) is covered on top of polymer and then the sample is flipped over in ultrapure water. (d) Single layer graphene on top of target polymer. (A color version of this figure can be viewed online.)

stage for movement and the step size was set to be 1 μm for both *x* and *y* directions. It took about 27 h for each mapping.

The C K-edge NEXAFS experiments were performed at Beamline 8.0.1 at the Advanced Light Source (ALS), Lawrence Berkeley National Laboratory (LBNL), USA. This beamline is connected with a 5 cm period undulator and covers photons with energy ranging from 80 to 1250 eV. The total electron yield (TEY) mode was used for NEXAFS measurements and the signal was obtained by monitoring the sample drain current. The energy resolution was 0.1 eV. To avoid the possible beam damage, all the samples were measured at two-bunch time with a reduced beam flux. Before the NEXAFS experiments, the samples were annealed to 120 °C for 1 h to remove possible surface contaminants.

The SRPES experiments were carried out at Beamline 4D 1 PES II in Pohang Accelerator Laboratory, Korea. This bending magnet source delivers photons with an energy range from 200 to 1000 eV. The base pressure of the endstation analysis chamber is $\sim 5 \times 10^{-10}$ mbar. Al was in-situ deposited onto graphene/P3HT film by thermal evaporation at an average deposition rate of 0.6 nm/min. All SRPES spectra were taken at normal emission. In addition, UPS measurements were also performed at the same samples and He I with the photon energy of 21.2 eV was used as the light source.

3. Results and discussion

3.1. *Raman measurements*

We first transferred CVD-grown single layer graphene onto PMMA using the procedure shown in Fig. 1. The structural property of the graphene/PMMA sample was investigated with Raman measurements and the results are shown in Fig. 2. It should be mentioned that we used PMMA instead of P3HT for Raman experiments because the high luminescence background from P3HT generated by 532 nm wavelength light excitation is thousands of times stronger than the peak intensity of graphene, making it difficult to collect signals from single layer graphene (see Fig. S1). Fig. 2a presents the 100 μm × 100 μm optical image of the graphene/PMMA sample. The presence of defects and number of graphene layers can be identified using Raman spectroscopy [36,37]. The black line in Fig. 2b is the Raman spectrum of the graphene/PMMA sample from the center spot of Fig. 2a. Compared with the Raman spectrum of pure PMMA (red line), several peaks which are typical for graphene can be observed, as labeled on top of the spectrum. The intensity of 2D peak (~2684 cm^{-1}) is more than two times stronger than that of G peak (~1591 cm^{-1}), and, moreover, this 2D peak can be perfectly fitted by one Lorenz peak [38,39], suggesting that the graphene on top of PMMA is single layer [38]. Note that a red shift (~3 cm^{-1}) of the 2D peak for graphene/PMMA (~2684 cm^{-1}) as compared to the 2D peak for as-grown graphene on Cu (~2687 cm^{-1}) (as shown in Fig. S2) may be attributed to a very weak strain, if it presents, between graphene and PMMA [38–42]. In addition, the D peak (~1340 cm^{-1}), which is ascribed to the breathing mode of sp^2 atoms and activated by the existence of defect states [38], can hardly be observed, providing strong evidence that this transfer process does not introduce too many defects in graphene. Furthermore, the appearance of the very intense 2D peak (~3246 cm^{-1}) further confirms that the graphene possess high sp^2 hybridized crystalline quality [43].

We also performed the Raman mapping experiment within the same area of Fig. 2a and the corresponding results are summarized in Fig. 2c–f. As can be seen in Fig. 2c, the I_{2D}/I_G ratio over the entire area is much greater than 1. Therefore, the graphene samples on top of PMMA are indeed single layer

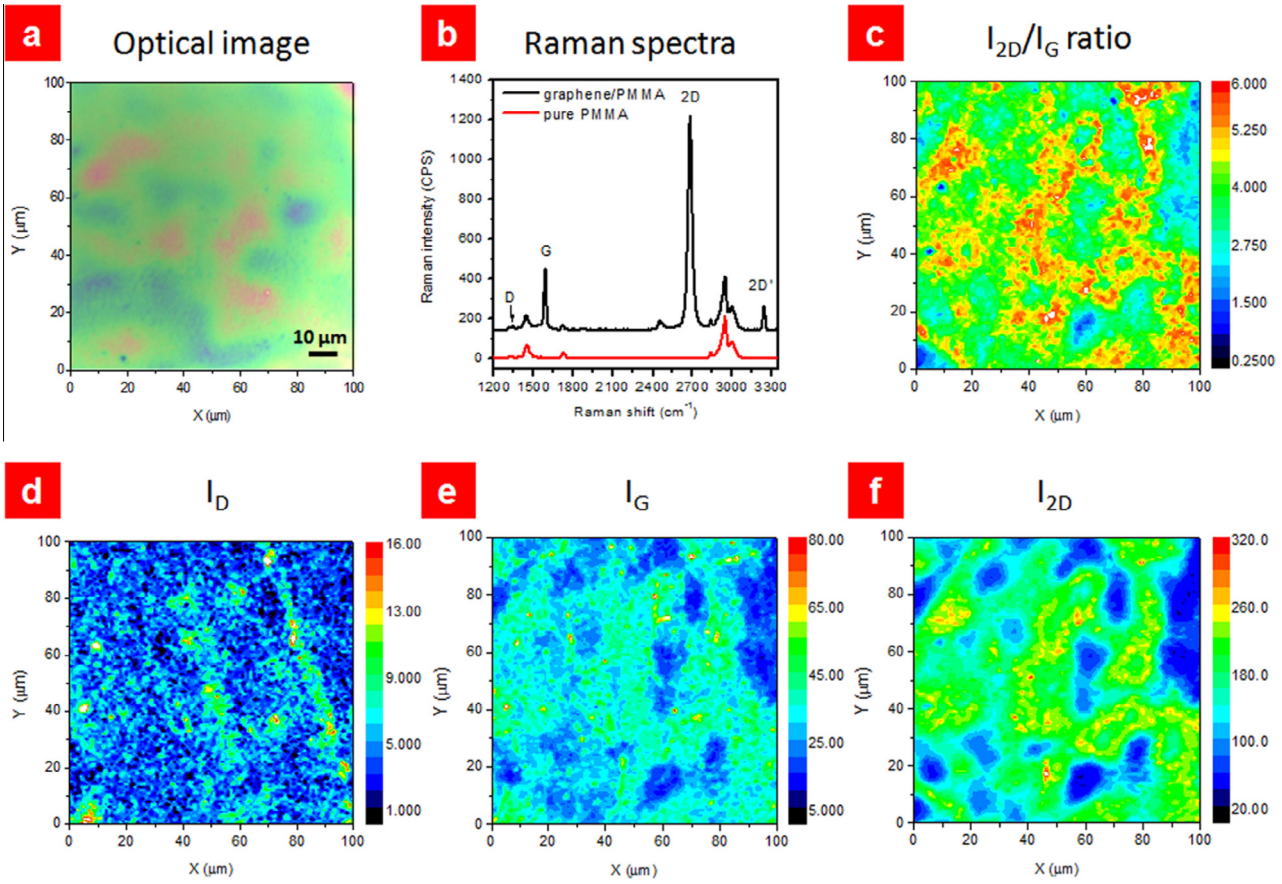

Fig. 2 – (a) Optical image of 100 μm × 100 μm graphene/PMMA film, (b) Raman spectra of graphene/PMMA and pure PMMA obtained with 532 nm excitation, (c)–(f): I_{2D}/I_G, I_D, I_G and I_{2D} Raman maps over the same area of the optical image. (A color version of this figure can be viewed online.)

[44]. In addition, the intensity of D peak (Fig. 2d) is much lower than those of G peak (Fig. 2e) and 2D peak (Fig. 2f) in the whole measured area, revealing that most of the PMMA surface is covered with high quality single layer graphene, although a few defects can be induced during the growth and/or graphene transfer process.

3.2. *Angle-dependent NEXAFS measurements*

Due to the fact that the graphene/P3HT system is not suitable for Raman measurements, as explained above, we employed NEXAFS to identify the structural difference of the P3HT films with/without graphene on top. Fig. 3a–c show the surface-sensitive, TEY mode angle-dependent C K-edge NEXAFS spectra from the samples of graphene, pure P3HT and graphene/P3HT on Si wafers, respectively. The graphene/Si wafer sample was prepared using a conventional PMMA-supported transfer method, as described in our previous study [38]. As can be seen in Fig. 3a, the features at 285.5, 291.8 and 292.7 eV can be attributed to the transitions from the C 1s core level to the π^*, excitonic and σ^* states of graphene, respectively [38]. For the spectra of pure P3HT (Fig. 3b), the peak at 285.4 eV can be attributed to the transition from C 1s to the π^* state, while the features at 287.0 and 292.5 eV correspond to the transition from C 1s to the C–S/C–H and C–C σ^* states, respectively [45]. Compared with the spectra shown in Fig. 3a, except for the characteristic peak at 287.0 eV of P3HT, an obvious difference is that no sharp peak at 291.8 eV can be observed. Thus, the feature at 291.8 eV can be used as a fingerprint for the presence of graphene in our NEXAFS experiments.

As can be seen in Fig. 3c, in addition to the features of P3HT, signals from graphene are also observed for the graphene/P3HT/Si wafer sample. Firstly, the fingerprint peak of graphene at 291.8 eV is observed. Secondly, in contrast to the C K-edge spectrum of pure P3HT, the intensities of C 1s to π^* and σ^* change significantly with X-ray incident angle, which is similar to that of graphene. These two observations provide a clear evidence of the presence of graphene on P3HT. In addition, we have used the same procedure to transfer graphene onto poly(9,9-dioctylfluorene-co-benzothiadiazole) (F8BT) and similar results has been achieved (see Fig. S3 for detail). Thus, we can confirm that this transfer approach is suitable for transferring single layer graphene on any polymer organic materials besides PMMA, such as P3HT and F8BT.

In contrast to the conventional transfer methods using foreign supporting materials for graphene transfer, there are three advantages for the present approach: (1) by using the target polymer organic materials as the supporting materials, the transfer procedure is simplified since no transfer material

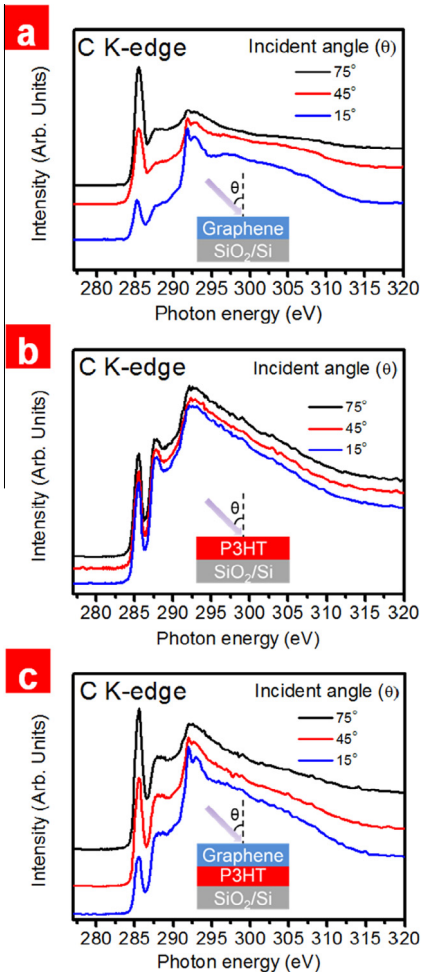

Fig. 3 – TEY mode C K-edge NEXAFS spectra of (a) pure graphene, (b) pure P3HT and (c) graphene/P3HT on top of Si wafers at different incident angles (θ). The inserts show the schematic drawings of samples used in the angle-dependent NEXAFS experiments. (A color version of this figure can be viewed online.)

removal is needed besides etching away the Cu substrate for graphene growth. (2) Transfer-induced contaminants can be minimized. (3) This heating- and organic solvent-free transfer method is prone for transferring graphene on organic materials, because many organic materials are soluble in organic solvents (i.e., acetone) or can be damaged or degraded when heated to high temperatures. Therefore, this transfer approach is feasible to obtain high-quality graphene on top of organic materials.

3.3. *In-situ SRPES experiments on Al/P3HT and Al/graphene/P3HT interfaces*

In order to study the influence of single layer graphene insertion on the interface structure between metal electrode and polymer organic material, which is the common interface in the polymer based organic electronic and optoelectronic devices, we utilized in-situ SRPES measurements to investigate the interface formation of Al with pure P3HT and graphene/P3HT on Si wafer samples. To minimize the possible variation of Al deposition, we mounted the two samples on the same sample holder in parallel and deposited Al at the same time. Moreover, to increase the surface sensitivity, we used the photon energies to be 50–100 eV higher than the binding energies of the measured core-levels (e.g., $h\nu$ = 250 eV for S 2p) [46].

Fig. 4 shows the S 2p SRPES spectra from the samples of pure P3HT and graphene/P3HT on Si wafers deposited with different thicknesses of Al at 300 K, namely, 0, 0.04 and 0.7 nm. Before Al deposition, the intensity of S 2p from graphene/P3HT (Fig. 4d) is about 5 times weaker than that of pure P3HT (Fig. 4d) due to the damping effect of the single layer graphene on top of the P3HT. In addition, the S 2p peak shifts by 0.4 eV towards the lower binding energy side compared with that of pure P3HT, implying the formation of an upward band bending induced by electron transfer from P3HT to graphene. Similar phenomenon was also reported at the F4-TCNQ/graphene interface [47].

After 0.04 nm Al deposition, both the original S 2p peaks (labeled as "unreacted" S) of P3HT and graphene/P3HT shift slightly to higher binding energy side by 0.1 eV, which is attributed to the downward band bending due to the electron transfer from Al to the underlying substrate films. Similar band bending phenomena have also been observed for Ca/P3HT [48,49] and Li/P3HT [46]. In addition, a new doublet feature at a binding energy of 1.5 eV lower than the original peak (the blue shaded area, labeled as "reacted" S) appears (Fig. 4b and e). This can be attributed to the strong chemical reactions between Al and P3HT, leading to the formation of Al-thiophene (Al-T) complex [50]. In contrast to Al/P3HT interface, the intensity of this new peak from Al/graphene/P3HT is significantly weaker, suggesting that the chemical reaction between Al and P3HT with the existence of single layer graphene has been reduced.

Further deposition of Al to 0.7 nm leads to the total S 2p signal damping and increased intensity of "reacted" S component on both P3HT and graphene/P3HT surfaces, suggesting that on both surfaces, part of the deposited Al stays on top of the surface and part of them diffuses to subsurface to continue the chemical reaction of Al with P3HT. However, by comparing the S 2p spectra on both surfaces, it can be clearly seen that on the P3HT surface, the intensity ratio between "unreacted" S to "reacted" S is much smaller than that on the graphene/P3HT surface (22:78 in Fig. 4c to 62:38 in Fig. 4f), implying that the single layer graphene can effectively prevent the diffusion of Al atoms into P3HT and the interfacial chemical reaction between Al and P3HT is suppressed significantly. Generally speaking, the strong interfacial chemical reactions between low-work-function metal electrodes and organic materials are usually detrimental for the stability and lifetime of organic electronic device [51]. Therefore, the insertion of such a graphene layer between metal electrodes and active organic materials is helpful to obtain a sharp and stable metal/organic interface. In addition, on the graphene/P3HT surface the deposition of 0.7 nm Al leads to the shift of S 2p spectrum towards lower binding energy side by 0.4 eV, which may be caused by the formation of a downward interface dipole between the top Al layer and the underlying graphene/P3HT substrate.

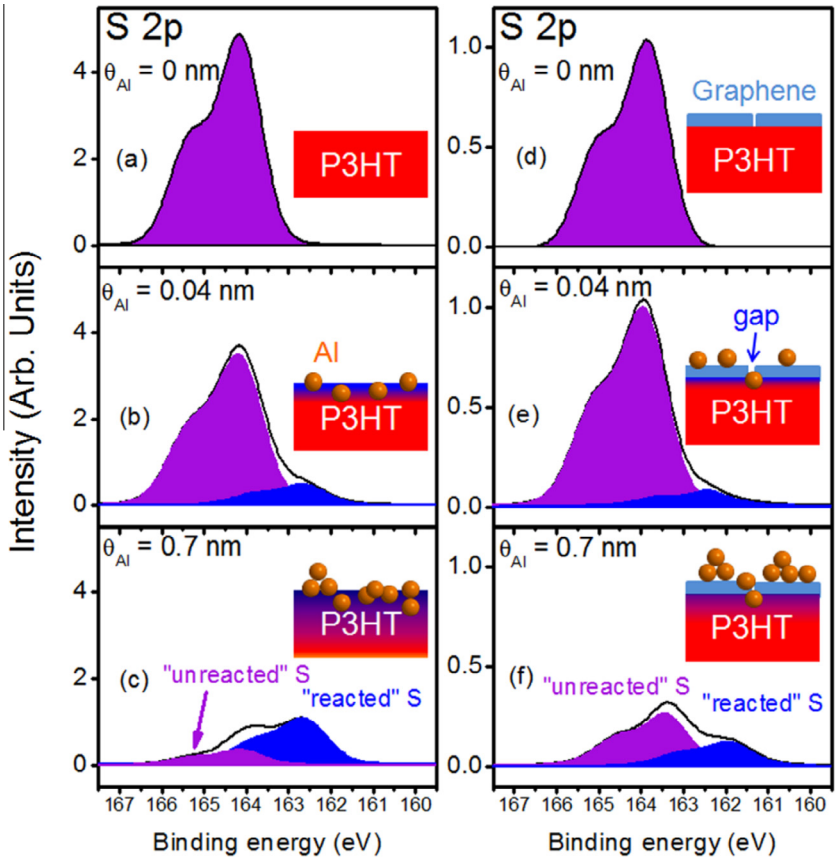

Fig. 4 – S 2p SRPES spectra ($h\nu$ = 250 eV) of pure P3HT (a), P3HT with 0.04 nm (b) and 0.7 nm (c) Al deposited on the surface, respectively. The S 2p spectra of graphene/P3HT with the same Al thicknesses are presented in (d)–(f) for comparison. The purple shaded area (left) and blue shaded area (right) are attributed to unreacted P3HT and P3HT reacted with Al, which are labeled "unreacted" S and "reacted" S, respectively. The inserts are simplified models of Al/P3HT and Al/graphene/P3HT interfaces. The photoelectron detection angle relative to the surface normal is 0°. (A color version of this figure can be viewed online.)

Note that structural defects commonly exist during the CVD growth of graphene on Cu foil [52]. In addition, defects can also be introduced during transferring, leading to the fact that not all the P3HT surface is covered by single layer graphene. This can be the major reason why chemical reaction between Al and P3HT still occurs at Al/graphene/P3HT interface, although the extent of reaction has been reduced significantly.

3.4. *In-situ UPS measurements on Al/P3HT and Al/graphene/P3HT interfaces*

Fig. 5a–d present the UPS spectra of Al/P3HT and Al/graphene/P3HT interfaces, respectively. The detailed explanation of the UPS spectra of P3HT can be found in our previous studies [46]. For pure P3HT, the work function is 3.36 eV, as determined from the width of the UPS spectrum. When P3HT is covered with a single layer graphene, the work function increases to 3.91 eV. Meanwhile, the band bends upwards by 0.4 eV, judged from the shift of S 2p binding energy. It is well-known that by subtracting the band bending effect from the work function change, a local interface dipole can be obtained. This yields a 0.15 eV interface dipole formation after transferring a single layer graphene on top of P3HT. The direction of this interface dipole is from P3HT to graphene (upward), indicating charge transfer from P3HT to single layer graphene.

After Al was deposited on both P3HT and graphene/P3HT sample surfaces, both the work functions decreased. When 0.04 nm Al was deposited on both films, the work function decreases 0.02 and 0.36 eV for Al/P3HT and Al/graphene/P3HT, respectively. Taking the band bending (again judged from the S 2p binding energy shift) into account, the interface dipoles at Al/P3HT and Al/graphene/P3HT interfaces can be calculated to be 0.08 and −0.26 eV, respectively. Similarly, after 0.7 nm Al deposition, the interface dipoles change to 0.06 and 0.03 eV for the two samples, respectively. These results indicate that with the insertion of single-layer graphene, it is possible to control the interface dipole direction by controlling the Al thickness. In addition, with very low Al coverages, a downward interface dipole at Al/graphene/P3HT interface can be formed, while there is almost no dipole at Al/P3HT interface. The formation of a downward interface dipole can reduce the barrier for electron transfer from

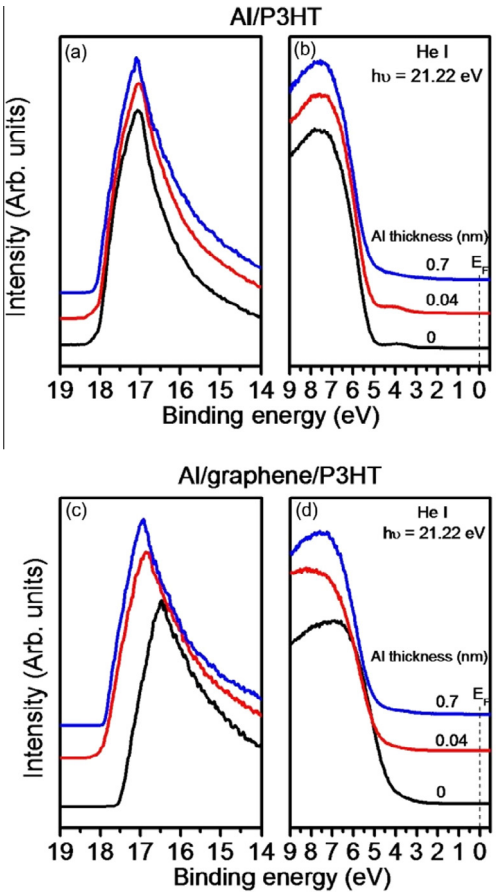

Fig. 5 – UPS spectra of Al/P3HT and Al/graphene/P3HT interfaces. The thicknesses of Al on P3HT and graphene/P3HT are 0, 0.04 and 0.7 nm. (A color version of this figure can be viewed online.)

organic layer to cathode, which may be helpful for increasing the organic solar cell efficiency.

4. Conclusions

In summary, we have developed a new approach that enables us to transfer single layer graphene on top of organic polymer materials. By directly using the target organic materials as the supporting materials for graphene suspension, this simple, heating- and organic solvent-free transfer method makes it possible to obtain high-quality and single layer graphene/organic interface with minimized contaminants. It is demonstrated that the single layer graphene, acting as a buffer layer between metal electrodes and organic functional materials, can significantly reduce the metal diffusion into the organic subsurface and the reaction with the organic materials. Moreover, the insertion of a single layer graphene between metal cathode and organic functional layer enables us to tune the metal/organic interfacial electronic structure via controlling the cathode thickness. We hope the information we have gained in this study will help to optimally design novel organic (opto-)electronic devices with longer lifetime and high stability.

Acknowledgements

This work is financially supported from the National Basic Research Program of China (2013CB834605), the National Natural Science Foundation of China (21173200, 21473178), the NSFC–NRF Scientific Cooperation Program (21211140238), and the Specialized Research Fund for the Doctoral Program of Higher Education of Ministry of Education (20113402110029). The Advanced Light Source is supported by the Director, Office of Science, Office of Basic Energy Sciences, of the U.S. Department of Energy under Contract No. DE-AC02-05CH11231. We would like to acknowledge Prof. Zhi Liu in the State Key Laboratory of Functional Materials for Informatics, Shanghai Institute of Microsystem and Information Technology, Chinese Academy of Sciences for his helpful discussions.

Appendix A. Supplementary data

Supplementary data associated with this article can be found, in the online version, at http://dx.doi.org/10.1016/j.carbon.2015.01.059.

REFERENCES

[1] Li N, Oida S, Tulevski GS, Han SJ, Hannon JB, Sadana DK, et al. Efficient and bright organic light-emitting diodes on single-layer graphene electrodes. Nat Commun 2013;4:3294–300.
[2] Han TH, Lee Y, Choi MR, Woo SH, Bae SH, Hong BH, et al. Extremely efficient flexible organic light-emitting diodes with modified graphene anode. Nat Photonics 2012;6:105–10.
[3] Meng H, Luo JX, Wang W, Shi ZJ, Niu QL, Dai L, et al. Top-emission organic light-emitting diode with a novel copper/graphene composite anode. Adv Funct Mater 2013;23:3324–8.
[4] Lu CC, Lin YC, Yeh CH, Huang JC, Chiu PW. High mobility flexible graphene field-effect transistors with self-healing gate dielectrics. ACS Nano 2012;6:4469–74.
[5] Park SJ, Kwon OS, Lee SH, Song HS, Park TH, Jang J. Ultrasensitive flexible graphene based field-effect transistor (FET)-type bioelectronic nose. Nano Lett 2012;12:5082–90.
[6] He RX, Lin P, Liu ZK, Zhu HW, Zhao XZ, Chan HLW, et al. Solution-gated graphene field effect transistors integrated in microfluidic systems and used for flow velocity detection. Nano Lett 2012;12:1404–9.
[7] Lemaitre MG, Donoghue EP, McCarthy MA, Liu B, Tongay S, Gila B, et al. Improved transfer of graphene for gated schottky-junction, vertical, organic, field-effect transistors. ACS Nano 2012;6:9095–102.
[8] Li XS, Cai WW, An JH, Kim S, Nah J, Yang DX, et al. Large-area synthesis of high-quality and uniform graphene films on copper foils. Science 2009;324:1312–4.
[9] Liu ZK, Li JH, Yan F. Package-free flexible organic solar cells with graphene top electrodes. Adv Mater 2013;25:4296–301.
[10] Park H, Chang S, Jean J, Cheng JJ, Araujo PT, Wang MS, et al. Graphene cathode-based ZnO nanowire hybrid solar cells. Nano Lett 2013;13:233–9.
[11] Yun JM, Yeo JS, Kim J, Jeong HG, Kim DY, Noh YJ, et al. Solution-processable reduced graphene oxide as a novel alternative to PEDOT:PSS hole transport layers for highly efficient and stable polymer solar cells. Adv Mater 2011;23:4923–8.

[12] Pang SP, Hernandez Y, Feng XL, Mullen K. Graphene as transparent electrode material for organic electronics. Adv Mater 2011;23:2779–95.
[13] Hecht DS, Hu LB, Irvin G. Emerging transparent electrodes based on thin films of carbon nanotubes, graphene, and metallic nanostructures. Adv Mater 2011;23:1482–513.
[14] Ellmer K. Past achievements and future challenges in the development of optically transparent electrodes. Nat Photonics 2012;6:808–16.
[15] Panwar OS, Kumar Kesarwani A, Dhakate SR, Singh BP, Rakshit RK, et al. Few layer graphene synthesized by filtered cathodic vacuum arc technique. J Vac Sci Technol B 2013;31:040602.
[16] Kesarwani AK, Panwar OS, Chockalingam S, Bisht A, Dhakate SR, Singh BP, et al. Graphene synthesized from solid carbon source using filtered cathodic vacuum arc technique for transparent conducting and field effect transistor devices. Sci Adv Mater 2014;6:2124–33.
[17] Yu QK, Jauregui LA, Wu W, Colby R, Tian JF, Su ZH, et al. Control and characterization of individual grains and grain boundaries in graphene grown by chemical vapour deposition. Nat Mater 2011;10:443–9.
[18] Bhaviripudi S, Jia XT, Dresselhaus MS, Kong J. Role of kinetic factors in chemical vapor deposition synthesis of uniform large area graphene using copper catalyst. Nano Lett 2010;10:4128–33.
[19] Vlassiouk I, Regmi M, Fulvio PF, Dai S, Datskos P, Eres G, et al. Role of hydrogen in chemical vapor deposition growth of large single-crystal graphene. ACS Nano 2011;5:6069–76.
[20] Li XS, Magnuson CW, Venugopal A, An JH, Suk JW, Han BY, et al. Graphene films with large domain size by a two-step chemical vapor deposition process. Nano Lett 2010;10:4328–34.
[21] Regmi M, Chisholm MF, Eres G. The effect of growth parameters on the intrinsic properties of large-area single layer graphene grown by chemical vapor deposition on Cu. Carbon 2012;50:134–41.
[22] Kang J, Shin D, Bae S, Hong BH. Graphene transfer: key for applications. Nanoscale 2012;4:5527–37.
[23] Li XS, Zhu YW, Cai WW, Borysiak M, Han BY, Chen D, et al. Transfer of large-area graphene films for high-performance transparent conductive electrodes. Nano Lett 2009;9:4359–63.
[24] Liang XL, Sperling BA, Calizo I, Cheng GJ, Hacker CA, Zhang Q, et al. Toward clean and crackless transfer of graphene. ACS Nano 2011;5:9144–53.
[25] Caldwell JD, Anderson TJ, Culbertson JC, Jernigan GG, Hobart KD, Kub FJ, et al. Technique for the dry transfer of epitaxial graphene onto arbitrary substrates. ACS Nano 2010;4:1108–14.
[26] Reina A, Jia XT, Ho J, Nezich D, Son HB, Bulovic V, et al. Large area, few-layer graphene films on arbitrary substrates by chemical vapor deposition. Nano Lett 2009;9:30–5.
[27] Lock EH, Baraket M, Laskoski M, Mulvaney SP, Lee WK, Sheehan PE, et al. High-quality uniform dry transfer of graphene to polymers. Nano Lett 2012;12:102–7.
[28] Pirkle A, Chan J, Venugopal A, Hinojos D, Magnuson CW, McDonnell S, et al. The effect of chemical residues on the physical and electrical properties of chemical vapor deposited graphene transferred to SiO_2. Appl Phys Lett 2011;99:122108–10.
[29] Bae S, Kim H, Lee Y, Xu XF, Park JS, Zheng Y, et al. Roll-to-roll production of 30-inch graphene films for transparent electrodes. Nat Nanotechnol 2010;5:574–8.
[30] Lin YC, Lu CC, Yeh CH, Jin CH, Suenaga K, Chiu PW. Graphene annealing: how clean can it be? Nano Lett 2012;12:414–9.
[31] Jeong HJ, Kim HY, Jeong SY, Han JT, Baeg KJ, Hwang JY, et al. Improved transfer of chemical-vapor-deposited graphene through modification of intermolecular interactions and solubility of poly(methylmethacrylate) layers. Carbon 2014;66:612–8.
[32] Song HS, Li SL, Miyazaki H, Sato S, Hayashi K, Yamada A, et al. Origin of the relatively low transport mobility of graphene grown through chemical vapor deposition. Sci Rep 2012;2:337–42.
[33] Ni ZH, Yu T, Luo ZQ, Wang YY, Liu L, Wong CP, et al. Probing charged impurities in suspended graphene using Raman spectroscopy. ACS Nano 2009;3:569–74.
[34] Tamaoki M, Imaeda H, Kishimoto S, Mizutani T. Transfer-free fabrication of graphene field effect transistor arrays using solid-phase growth of graphene on a SiO_2/Si substrate. Appl Phys Lett 2013;103:183114–6.
[35] Sokolov DA, Shepperd KR, Orlando TM. Formation of graphene features from direct laser-induced reduction of graphite oxide. J Phys Chem Lett 2010;1:2633–6.
[36] Buron JD, Petersen DH, Boggild P, Cooke DG, Hilke M, Sun J, et al. Graphene conductance uniformity mapping. Nano Lett 2012;12:5074–81.
[37] Kataria S, Patsha A, Dhara S, Tyagi AK, Barshilia HC. Raman imaging on high-quality graphene grown by hot-filament chemical vapor deposition. J Raman Spectrosc 2012;43:1864–7.
[38] Zhang L, Pollak E, Wang WC, Jiang P, Glans PA, Zhang YG, et al. Electronic structure study of ordering and interfacial interaction in graphene/Cu composites. Carbon 2012;50:5316–22.
[39] Wang YY, Ni ZH, Yu T, Shen ZX, Wang HM, Wu YH, et al. Raman studies of monolayer graphene: the substrate effect. J Phys Chem C 2008;112:10637–40.
[40] Gong L, Kinloch IA, Young RJ, Riaz I, Jalil R, Novoselov KS. Interfacial stress transfer in a graphene monolayer nanocomposite. Adv Mater 2010;22:2694–7.
[41] Zhang L, Zhang XG, Chen Y, Su JN, Liu WW, Zhang TH, et al. Interfacial stress transfer in a graphene nanosheet toughened hydroxyapatite composite. Appl Phys Lett 2014;105:161908.
[42] Pan Y, Gao Y, Kong D, Wang G, Hou J, Hu S, et al. Interaction of Au with thin ZrO2 films: influence of ZrO2 morphology on the adsorption and thermal stability of Au nanoparticles. Langmuir 2012;28:6045–51.
[43] Annamalai M, Mathew S, Jamali M, Zhan D, Palaniapan M. Elastic and nonlinear response of nanomechanical graphene devices. J Micromech Microeng 2012;22:105024–34.
[44] Ferrari JCM AC, Scardaci V, Casiraghi C, Lazzeri M, Mauri F, Piscanec S, et al. Raman spectrum of graphene and graphene layers. Phys Rev Lett 2006;97:187401–4.
[45] Chua LL, Dipankar M, Sivaramakrishnan S, Gao XY, Qi DC, Wee ATS, et al. Large damage threshold and small electron escape depth in X-ray absorption spectroscopy of a conjugated polymer thin film. Langmuir 2006;22:8587–94.
[46] Feng XF, Zhao W, Ju HX, Zhang L, Zhang WH, Zhu JF. Electronic structures and chemical reactions at the interface between Li and regioregular poly (3-hexylthiophene). Org Electron 2013;13:1060–7.
[47] Coletti C, Riedl C, Lee DS, Krauss B, Patthey L, Klitzing Kv. Charge neutrality and band-gap tuning of epitaxial graphene on SiC by molecular doping. Phys Rev B 2010;81:235401–8.
[48] Zhu JF, Bebensee F, Hieringer W, Zhao W, Baricuatro JH, Farmer JA, et al. Formation of the calcium/poly(3-Hexylthiophene) interface: structure and energetics. J Am Chem Soc 2009;131:13498–507.

[49] Zhao W, Guo YX, Feng XF, Zhang L, Zhang WH, Zhu JF. Electronic structure and chemical reaction of Ca deposition on regioregular poly(3-hexylthiophene) surfaces. Chin Sci Bull 2009;54:1978–82.
[50] Salaneck WR, Bredas JL. The metal-on-polymer interface in polymer light emitting diodes. Adv Mater 1996;8:48–52.
[51] Turak A. Interfacial degradation in organic optoelectronics. RSC Adv 2013;3:6188–225.
[52] Muñoz R, Gómez-Aleixandre C. Review of CVD synthesis of graphene. Chem Vap Deposition 2013;19:297–322.